Spin-Electric Coupling in Molecular Magnets

Mircea Trif,[1] Filippo Troiani,[2] Dimitrije Stepanenko,[1] and Daniel Loss[1]

[1]*Department of Physics, University of Basel, Klingelbergstrasse 82, CH-4056 Basel, Switzerland*

[2]*CNR-INFM National Research Center S3 c/o Dipartimento di Fisica via G. Campi 213/A, 41100, Modena, Italy*

(Received 8 May 2008; published 20 November 2008)

We study the triangular antiferromagnet Cu_3 in external electric fields, using symmetry group arguments and a Hubbard model approach. We identify a spin-electric coupling caused by an interplay between spin exchange, spin-orbit interaction, and the chirality of the underlying spin texture of the molecular magnet. This coupling allows for the electric control of the spin (qubit) states, e.g., by using an STM tip or a microwave cavity. We propose an experimental test for identifying molecular magnets exhibiting spin-electric effects.

DOI: 10.1103/PhysRevLett.101.217201 PACS numbers: 75.50.Xx, 03.67.Lx

Single-molecule magnets (SMMs) [1] have emerged as a fertile testing ground for investigating quantum effects at the nanoscale, such as tunneling of magnetization [2,3], or coherent charge transport [4–6], or the decoherence and the transition from quantum to classical behavior [7]. SMMs with antiferromagnetic coupling between spins are especially promising for the encoding and manipulation of quantum information [8–11], for they act as effective two-level systems, while providing additional auxiliary states that can be exploited for performing quantum gates. Intra- and intermolecular couplings of SMMs can be engineered by molecular and supramolecular chemistry [12], enabling a bottom-up design of molecule-based devices [13].

While the properties of SMMs can be chemically modified, the fast control required for quantum information processing remains a challenge. The standard spin-control technique is electron spin resonance (ESR) driven by ac magnetic fields $B_{ac}(t)$ [7]. For manipulation on the time scale of 1 ns, B_{ac} should be of the order of 10^{-2} T, which, however, is difficult to achieve. The spatial resolution of 1 nm, required for addressing a single molecule, is also prohibitively small. At these spatial and temporal scales, the electric control is preferable, because strong electric fields can be applied to small regions by using, for example, STM tips [14,15], see Fig. 1(a). Also, the quantized electric field inside a microwave cavity can be used [16–19] to control single qubits and to induce coupling between them even if they are far apart. Electric control of spins has been studied in multiferroic materials [20] and semiconductor spintronics [21], focusing on the control of a large number of spins and producing macroscopic magnetization and spin currents. Here, we are interested in control over a single molecular spin system.

We identify and study an efficient spin-electric coupling mechanism in SMMs which is based on an interplay of spin exchange, spin-orbit interaction (SOI), and lack of inversion symmetry. Spin-electric effects induced solely by SOI have been proposed [22] and experimentally demonstrated [23] in quantum dots. However, these SOI effects scale with the system size L as L^3 [22], making them irrelevant for the much smaller SMMs. Thus, additional ingredients-such as broken symmetries- must be present in SMMs for an efficient coupling between spin and applied electric field.

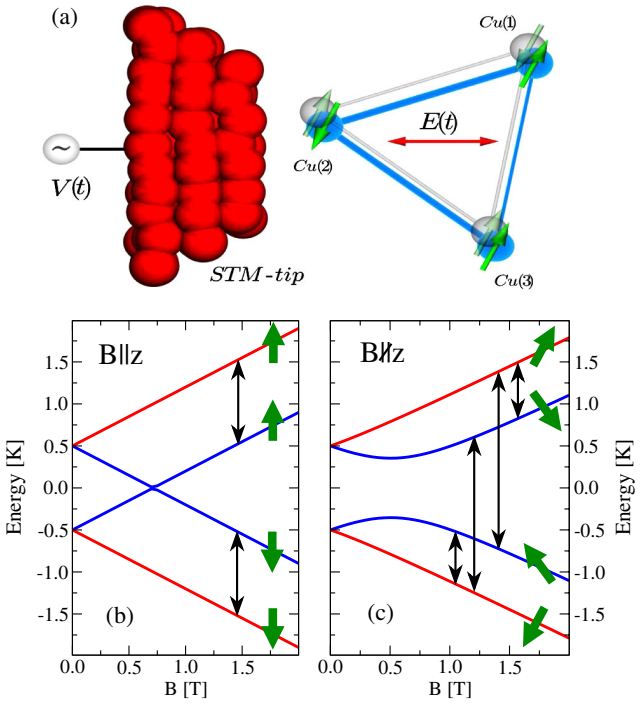

FIG. 1 (color online). (a) Cu_3-triangle exposed to an electric field $\mathbf{E}(t)$ created by, e.g., an STM-tip. For $\mathbf{E} = 0$, the exchange couplings, represented by the thickness of Cu-Cu bonds, are equal (light triangle). A finite $\mathbf{E}$ affects the (super-) exchange coupling in a directional way (dark triangle). (b),(c) Low-energy $S = 1/2$ states of Cu_3 in a magnetic field $\mathbf{B}$, with the zero-field SOI splitting $\Delta_{SO} = 1$ K. Light (red) and dark (blue) lines represent the states with $\chi = +1(-1)$. If $\mathbf{B} \parallel z$ (b), the transitions induced by $\mathbf{E}$ (thin arrows) conserve S_z; for $\mathbf{B} \nparallel z$ (c), these transitions result in a change of spin orientation (thick arrows).

In the following, we demonstrate the possibility of such spin-electric effects in SMMs by focusing on a specific example, namely, an equilateral spin triangle, Cu_3 [24]. In this SMM, the low-energy states exhibit a chiral spin texture and, due to the absence of inversion symmetry, electric fields couple states of opposite chirality. Moreover, SOI couples the chirality to the total spin, and thus an effective spin-electric interaction eventually emerges.

Spin-electric coupling.—At low energies, the Cu_3 can be described in terms of an effective spin Hamiltonian. There, the states are labeled by the quantum numbers of three spins-1/2 $\mathbf{s}_i$ (one for each Cu^{2+} ion), and the orbital states are quenched. The (super-) exchange and SOI are then expressed as Heisenberg and Dzyaloshinski-Moriya interaction of spins, [24],

$$H_0 = \sum_{i=1}^{3} J_{ii+1}\mathbf{s}_i \cdot \mathbf{s}_{i+1} + \sum_{i=1}^{3} \mathbf{D}_{ii+1} \cdot \mathbf{s}_i \times \mathbf{s}_{i+1}. \quad (1)$$

The D_{3h} symmetry of the triangle implies several relations between the coupling constants [25]. We neglect the intrinsic deformation of Cu_3 triangle that makes one of the sides slightly shorter. Since $J_{pq} \sim 5$ K and $|\mathbf{D}_{pq}| \sim 0.5$ K, the Heisenberg terms determine the gross structure of the energy spectrum, and the Dzyaloshinski-Moriya terms the fine one. In particular, since $J_{pq} > 0$, the ground state multiplet has total spin $S = 1/2$, and the gap to the first excited $S = 3/2$ quadruplet is $\Delta_H \equiv 3J/2$. The $S = 1/2$ subspace is spanned by the symmetry-adapted states $|\chi, M\rangle$, i.e.,

$$|\pm 1, +1/2\rangle \equiv (|\downarrow\uparrow\uparrow\rangle + \epsilon_{\pm}|\uparrow\downarrow\uparrow\rangle + \epsilon_{\mp}|\uparrow\uparrow\downarrow\rangle)/\sqrt{3}, \quad (2)$$

$$|\pm 1, -1/2\rangle \equiv (|\uparrow\downarrow\downarrow\rangle + \epsilon_{\pm}|\downarrow\uparrow\downarrow\rangle + \epsilon_{\mp}|\downarrow\downarrow\uparrow\rangle)/\sqrt{3}, \quad (3)$$

with $\epsilon_{\pm} = e^{\pm i2\pi/3}$, that are simultaneous eigenstates of the chirality operator C_z and of S_z (total spin), for the respective eigenvalues χ and M. Here, we have introduced the chirality $\mathbf{C}$ with components

$$C_x = (-2/3)(\mathbf{s}_1 \cdot \mathbf{s}_2 - 2\mathbf{s}_2 \cdot \mathbf{s}_3 + \mathbf{s}_3 \cdot \mathbf{s}_1), \quad (4)$$

$$C_y = (2/\sqrt{3})(\mathbf{s}_1 \cdot \mathbf{s}_2 - \mathbf{s}_3 \cdot \mathbf{s}_1), \quad (5)$$

$$C_z = (4/\sqrt{3})\mathbf{s}_1 \cdot (\mathbf{s}_2 \times \mathbf{s}_3). \quad (6)$$

They satisfy $[C_k, C_l] = i2\epsilon_{kln}C_n$ and $[C_k, S_l] = 0$, and act as Pauli matrices in the $|\chi = \pm 1\rangle$ bases.

Next, we study the effect of an electric field $\mathbf{E}$ on the Cu_3-spins using general symmetry group arguments. The low-energy $|E'_{\pm}, S = 1/2\rangle$ ($|A'_2, S = 3/2\rangle$) spin-orbital states form two E' (four A'_2) irreducible representations (IRs) of D_{3h}, with the $S = 1/2$ states lower in energy [24,25]. The states $|E'_{\pm}, S_z\rangle$ transform in the same way as the chiral states $|\chi = \pm 1, S_z\rangle$, Eqs. (2) and (3), with orbitals localized on the Cu ions corresponding to the triangle vertices. An electric field $\mathbf{E}$ couples to Cu_3 via $e\mathbf{E} \cdot \mathbf{R}$, where e is the electron charge, and $\mathbf{R} = \sum_{j=1}^{3} \mathbf{r}_j$. The Z component of $\mathbf{R}$ transforms as A'_2 IR, while the components $X_{\pm} = \pm X + iY$ in the Cu_3 plane transform as the two-dimensional IR E'. From the Wigner-Eckart theorem, it follows that the only nonzero matrix elements of $\mathbf{R}$ are $e\langle E'_+, S_z|X_-|E'_-, S_z\rangle = e\langle E'_-, S_z|X_+|E'_+, S_z\rangle = 2id$, with d real denoting the electric dipole coupling. The resulting coupling between the $\mathbf{E}$-field and chirality in the spin-Hamiltonian model takes the compact form $\delta H_E = d\mathbf{E}' \cdot \mathbf{C}_{\parallel}$, where $\mathbf{E}' = \mathcal{R}_z(\phi)\mathbf{E}$ is rotated by $\phi = 7\pi/6 - 2\theta$ about z, and $\mathbf{C}_{\parallel} = (C_x, C_y, 0)$.

To emphasize that the spin-electric effect derived above is based on exchange, we reinterpret our results in terms of spin interactions. In an equilateral triangle, and in the absence of electric field, the spin Hamiltonian is given by Eq. (1) with equal exchange couplings $J_{i,i+1} \equiv J$. Using then Eqs. (4) and (5), we find

$$\delta H_E = \frac{4dE}{3} \sum_{i=1}^{3} \sin[2(1-i)\pi/3 + \theta]\mathbf{s}_i \cdot \mathbf{s}_{i+1}, \quad (7)$$

where θ is the angle between an in-plane $\mathbf{E}$-field and the vector $\mathbf{r}_{12}$ pointing from site 1 to 2. This form of δH_E shows that the $\mathbf{E}$-field lowers the symmetry by introducing direction-dependent corrections to the exchange couplings J_{ii+1}. E.g., if $\theta = \pi/2$, $\delta J_{23} = \delta J_{31} \neq \delta J_{12}$. Intrinsic deformation of the molecule can be described as an internal electric field $\mathbf{E}_{\mathrm{mol}}$, giving Eq. (7) with $\mathbf{E} \rightarrow \mathbf{E} + \mathbf{E}_{\mathrm{mol}}$. The lack of inversion symmetry is crucial for the linear spin-electric coupling, since the electric field $\mathbf{E}$ is odd under inversion, and the spin is even.

Next, we turn to the SOI. The most general form of SOI allowed by the D_{3h} symmetry reads, $H_{\mathrm{SO}} = \sum_{i=1}^{3}[\lambda_{\mathrm{SO}}^{\parallel} T_{A''_2} s_z^i + \lambda_{\mathrm{SO}}^{\perp}(T_{E''_+} s_-^i + T_{E''_-} s_+^i)]$, where $\lambda_{\mathrm{SO}}^{\perp}(\lambda_{\mathrm{SO}}^{\parallel})$ is the effective SOI coupling constant for the A''_2- ($E''_{\pm}$-) irreducible representation, and $T_{A''_2}$ ($T_{E''_{\pm}}$) is the corresponding irreducible tensor operator in the orbital space [25]. Using again symmetry group arguments, we find that the SOI Hamiltonian acting in the $S = 1/2$ subspace reads $\delta H_{\mathrm{SO}} = \Delta_{\mathrm{SO}} C_z S_z$, where $\Delta_{\mathrm{SO}} = \lambda_{\mathrm{SO}}^{\parallel}$. The states are therefore split into two Kramers doublets $|E'_{\pm}, S_z = \pm 1/2\rangle$ and $|E'_{\pm}, S_z = \mp 1/2\rangle$. Using Eq. (6), δH_{SO} can be reduced to the Dzyaloshinski-Moriya interaction, given in Eq. (1). The coupling to a magnetic field $\mathbf{B}$ is given by $\mathbf{B} \cdot \bar{\bar{g}} \cdot \mathbf{S}$, with the Bohr magneton absorbed in the $\bar{\bar{g}}$-tensor. Because of the D_{3h}-symmetry, $\bar{\bar{g}}$ is diagonal with components $g_{xx} = g_{yy} = g_{\perp}$ in the Cu_3-plane and $g_{zz} = g_{\parallel}$ normal to it.

Combining δH_E and δH_{SO}, we finally obtain the effective low-energy Hamiltonian in the presence of SOI and electric and magnetic fields,

$$H_{\mathrm{eff}}^{\mathrm{spin}} = \Delta_{\mathrm{SO}} C_z S_z + g_{\perp}\mathbf{B}_{\perp} \cdot \mathbf{S} + g_{\parallel} B_z S_z + d\mathbf{E}' \cdot \mathbf{C}_{\parallel}. \quad (8)$$

From this we see that an in-plane $\mathbf{E}$-field causes rotations

of the chirality pseudospin. To illustrate the role of $\mathbf{B}$, we focus on the case $\mathbf{E} \parallel \mathbf{r}_{31}$, giving $\delta H_E = -dEC_x$. For $\mathbf{B} \parallel z$, the eigenstates coincide with those of S_z, and thus $\mathbf{E}$ will not induce transitions between $|\pm, 1/2\rangle$ and $|\pm, -1/2\rangle$, but will do so in subspaces of given M; see Fig. 1. For $\mathbf{B} \nparallel z$, instead, the system eigenstates for $\mathbf{E} = 0$ are no longer eigenstates of S_z, and thus the electric-field induced transitions result in spin flips; see Fig. 1(c).

The form of spin Hamiltonian, Eq. (8), is set by symmetry alone, but a microscopic evaluation of electric dipole coupling d requires an *ab initio* approach which is beyond the scope of this work. However d can be directly accessed in experiments, e.g., by standard ESR measurements in static electric fields; see Fig. 2. We can estimate d, $|\mathbf{E}|$ and the spin-manipulation (Rabi) time resulting from Eq. (8) as follows. For d between $d_{\min} = 10^{-4} eR_{12}$ and $d_{\max} = eR_{12}$ and for $E \approx 10^2$ kV/cm, obtainable near an STM tip, see Fig. 1(a), the Rabi time is $\tau_{\text{Rabi}} \approx 0.1$–$10^3$ ps. The condition $dE \ll \Delta_H$ for the validity of $H_{\text{eff}}^{\text{spin}}$ in Eq. (8) provides another lower bound on the spin-manipulation time, namely $\tau_{\text{Rabi}}^{\min} \approx 10$ ps. The spin control is not affected by the time-independent $\mathbf{E}_{\text{mol}}$.

Hubbard approach.—In order to gain further insight into the interplay between the exchange interaction and the electric field $\mathbf{E}$, we introduce an N_s-site Hubbard model of the triangular spin chain, with Cu ions represented by the sites on the vertices and the bridging atoms by sites on the sides, see Fig. 3(a). The corresponding Hamiltonian reads, $H_{\text{H}} = \sum_{i,\sigma}[(U_i/2)n_{i,\sigma}n_{i,-\sigma} + \epsilon_i n_{i,\sigma} + (t_{ii+1}c_{i,\sigma}^{\dagger}c_{i+1,\sigma} + \text{H.c.})]$, where U_i is the repulsion on site i, t_{ii+1} the hopping matrix element, $\sigma = \uparrow, \downarrow$, and $\sum_{i,\sigma} n_i^{\sigma} = N_e$. The coupling of the system to $\mathbf{E}$ is

$$H_E = e\mathbf{E} \cdot \sum_{i,\sigma}[n_{i,\sigma}\mathbf{r}_i + (\tilde{\mathbf{r}}_{ii+1}c_{i,\sigma}^{\dagger}c_{i+1,\sigma} + \text{H.c.})]. \quad (9)$$

In the single-site terms, the expectation value of the electron position $\mathbf{r}$ in the Wannier state $|\phi_i\rangle$ is identified with the ion position $\mathbf{r}_i = \langle\phi_i|\mathbf{r}|\phi_i\rangle$. The two-site terms describe the electric-field assisted hopping of electrons between neighboring sites, with $\tilde{\mathbf{r}}_{ii+1} = \langle\phi_i|\mathbf{r}|\phi_{i+1}\rangle = (\alpha_{ii+1}^{\parallel} + \alpha^{\perp}\mathbf{e}_z\times)\mathbf{r}_{ii+1}$, and $\mathbf{r}_{ii+1} = \mathbf{r}_{i+1} - \mathbf{r}_i$. We now focus on the two main mechanisms giving antiferromagnetic coupling, namely, direct exchange and superexchange (models A and B, Fig. 2(a)] for $|t_{ij}| \ll U_i$. In both cases, the low-energy subspace ($\mathcal{S}_0$) is defined by the states ($|\alpha^0\rangle$) where the magnetic ions at the triangle vertices are singly occupied. For $E = 0$, the projection of these states onto $\mathcal{S}_0$ ($|\Psi_{1-8}^0\rangle$) coincides with the $S = 1/2$ and $S = 3/2$ eigenstates of the Heisenberg Hamiltonian. The degeneracy in the $S = 1/2$ multiplet is lifted by $\mathbf{E}$.

In Fig. 3(b), we show the overlap between the projected ground state $|\Psi_1^0\rangle$ and the $|S = 1/2, S_{12} = 0, 1\rangle$ states for a given S_z as function of the direction of $\mathbf{E}$ (angle θ). The results coincide with the ones from Eq. (7), for both models A and B. In addition, we find that the splitting ($\Delta_{21} \equiv E_2 - E_1$) between the two lowest energies varies by less than 5% with θ, in agreement with H_E^{spin} that predicts no θ-dependence at all.

In Fig. 3(c) we isolate the contribution to Δ_{21} arising from the single- and two-site terms. All these contributions scale linearly with $|\mathbf{E}|$ for every θ. The dependence of Δ_{21} on t, however, is model dependent. In particular, in model A, the contributions to Δ_{21} arising from the single- and two-site terms scale as $(t/U)^3$ and (t/U), respectively, and

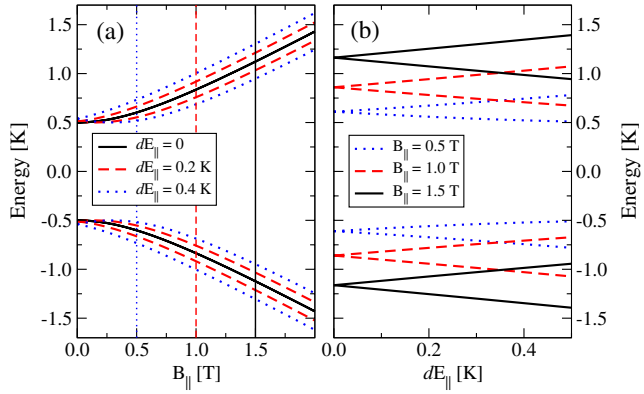

FIG. 2 (color online). Low-energy spectrum of the undeformed Cu_3 molecule. (a) Energy levels of the Cu_3 molecule in an in-plane magnetic field $B_{\parallel}$ (black solid line), split as a static in-plane electric field $E_{\parallel}$ is turned on (dashed red line and dotted blue line). (b) The electric dipole coupling d is given by the slope of energy levels as a function of $E_{\parallel}$ in a constant magnetic field [vertical lines in (a)]. Intrinsic deformation gives $\mathbf{E} \rightarrow \mathbf{E} + \mathbf{E}_{\text{mol}}$, allowing to measure $\mathbf{E}_{\text{mol}}$ as the field $\mathbf{E}$ at which the levels cross.

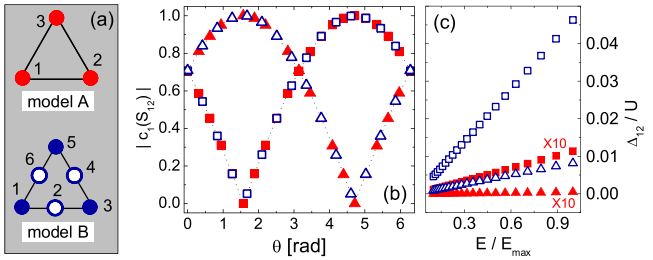

FIG. 3 (color online). (a) Hubbard models A and B of the spin triangle. Model A: $N_e = N_s = 3$, $t_i = t$, $U_i = U$, and $\epsilon_i = \alpha_{ii+1}^{\parallel} = 0$. Model B: $N_e = 9$, $N_s = 6$, $\alpha_{ii+1}^{\parallel} = 0$, $\alpha_{ii+1}^{\perp} = \alpha$, $t_i = t$, $\epsilon_{3k-2} - \epsilon_{3k'-1} = \epsilon$, $U_{3k-2} - U_{3k'-1} = U$ (k, $k' = 1$, 2, 3). (b) Overlap between the projected ground state of $H_H + H_E$ ($|\Psi_1^0\rangle$), and the eigenstates of $\mathbf{s}_1 \cdot \mathbf{s}_2$ with $S_{12} = 0$ (squares) and $S_{12} = 1$ (triangles), as function of the angle θ between the triangle side 1–2 and an in-plane $\mathbf{E}$. The filled (empty) symbols correspond to the A (B) model, whereas the dotted lines give the components of the δH_E ground state. In both models, $t/U = 0.1$, $eRE/U = 2.5 \times 10^{-2}$, and $\alpha = 0.1$. (c) Dependence of Δ_{21} on the amplitude E, for $\mathbf{E} \parallel y$ and $eRE_{\max}/U = 2.5 \times 10^{-2}$. Filled (empty) symbols refer to the A (B) model, and squares (triangles) to $\alpha = 0.1$ ($\alpha = 0$) two-site contributions.

$d = 4t|e\tilde{r}_{12}^{y}|/U$. Analogous power-law dependences are found in model B, where the single-site (two-site) contribution scales as $(t/U)^4$ ($(t/U)^3$, and two-site terms dominate in both models. Additional mechanisms, such as the relative displacements of the ions, can contribute to the coupling between spin and electric field.

Spin coupling to cavity electric fields.—Exchange coupling of SMMs has been demonstrated in dimers [26]. The use of this short-range and (so far) untunable interaction requires additional resources for quantum information processing [27]. Efficient spin-electric interaction, on the other hand, provides a route to long-range and switchable coupling between SMM qubits. In particular, microwave cavities are suitable for reaching the strong-coupling regime for various qubit systems [16–19]. Here, we propose to use such cavities to control single SMMs and, moreover, to couple the spin qubits of distant SMMs placed inside the same cavity.

The interaction of a single SMM with the cavity field reads, $\delta H_E = d\mathbf{E}_0' \cdot \mathbf{C}_{\parallel}(b^\dagger + b)$, where $\mathbf{E}_0'$ is the rotated electric field of amplitude $|\mathbf{E}_0| \propto \sqrt{\hbar\omega/\mathcal{V}}$ inside the cavity of volume $\mathcal{V}$ [17], and b is the annihilation operator for the photon mode of frequency ω. The low-energy Hamiltonian of N SMMs interacting with the cavity mode is $H_{s\text{-ph}} = \sum_j(\Delta_{\mathrm{SO}} C_z^{(j)} S_z^{(j)} + \mathbf{B}\cdot\bar{\bar{g}}\cdot\mathbf{S}^{(j)} + H_{\mathrm{int}}^{(j)}) + \omega b^\dagger b$, where

$$H_{\mathrm{int}}^{(j)} = dE_0(e^{i\varphi_j} C_{-}^{(j)} + e^{-i\varphi_j} C_{+}^{(j)})(b + b^\dagger), \qquad (10)$$

with $C_{\pm}^{(j)} = C_x^{(j)} \pm iC_y^{(j)}$and $\varphi_j = 7\pi/6 - 2\theta_j$. In the rotating wave approximation $H_{s\text{-ph}}$ reduces to the well-known Tavis-Cummings model [28] when the spins are in eigenstates of $S_z^{(j)}$, and $\mathbf{B} \parallel z$. However, if $\mathbf{B} \nparallel z$ it is possible to couple both chiralities and total spins of distant molecules. Typically, the electric fields in cavities are weaker, $|\mathbf{E}_0| \approx 1$ V/cm for $\hbar\omega \approx 0.1$ meV [19], than the ones near STM tips, thus giving $\tau_{\mathrm{Rabi}} \approx$ 0.01–100 μs. Obviously, decreasing the cavity volume $\mathcal{V}$ would give shorter τ_{Rabi}. Coupling of distant SMMs can be controlled by tuning two given molecules in and out of resonance with the cavity mode, e.g., by applying additional local electric fields. For example, when $\mathbf{B} = 0$ the coupling constant between distant molecules is $J \approx d^2E_0^2/(\Delta_{\mathrm{SO}} - \omega)$, with the typical chirality flipping time 0.05–500 μs. Further effects such as the state transfer between stationary and flying qubits, or the SMM-photon entanglement, can be observed in a system described by $H_{s\text{-ph}}$.

In conclusion, we find an exchange-based mechanism that couples electric fields to spins in triangular molecular antiferromagnets. While our results are derived for Cu_3, analogous symmetry arguments are expected to apply to other molecular magnets that lack inversion symmetry, such as V_{15} [29], Co_3 [30], Dy_3 [31], Mn_{12} [2,3], etc.

We thank D. Klauser, M. Affronte and V. Bellini for useful discussions. We acknowledge financial support from the Swiss NSF, the NCCR Nanoscience Basel; the Italian MIUR under FIRB Contract No. RBIN01EY74; the EU under MagMaNet, QuEMolNa and MolSpinQIP.

[1] D. Gatteschi, R. Sessoli, and J. Villain, *Molecular Nanomagnets* (Oxford Univ. Press, New York, 2007).
[2] J. R. Friedman *et al.*, Phys. Rev. Lett. **76**, 3830 (1996).
[3] L. Thomas *et al.*, Nature (London) **383**, 145 (1996).
[4] C. Romeike *et al.*, Phys. Rev. Lett. **96**, 196601 (2006).
[5] M. N. Leuenberger and E. R. Mucciolo, Phys. Rev. Lett. **97**, 126601 (2006).
[6] J. Lehmann and D. Loss, Phys. Rev. Lett. **98**, 117203 (2007).
[7] A. Ardavan *et al.*, Phys. Rev. Lett. **98**, 057201 (2007).
[8] M. Leuenberger and D. Loss, Nature (London) **410**, 789 (2001).
[9] F. Meier, J. Levy, and D. Loss, Phys. Rev. B **68**, 134417 (2003).
[10] F. Troiani *et al.*, Phys. Rev. Lett. **94**, 207208 (2005).
[11] J. Lehmann *et al.*, Nature Nanotech. **2**, 312 (2007).
[12] M. Affronte *et al.*, Angew. Chem., Int. Ed. **44**, 6496 (2005).
[13] L. Bogania and W. Wernsdorfer, Nature Mater. **7**, 179 (2008).
[14] C. F. Hirjibehedin, C. P. Lutz, and A. J. Heinrich, Science **312**, 1021 (2006).
[15] A. C. Bleszynski *et al.*, Phys. Rev. B **77**, 245327 (2008).
[16] A. Wallraff *et al.*, Nature (London) **431**, 162 (2004).
[17] G. Burkard and A. Imamoglu, Phys. Rev. B **74**, 041307 (2006).
[18] A. André *et al.*, Nature Phys. **2**, 636 (2006).
[19] M. Trif, V. N. Golovach, and D. Loss, Phys. Rev. B **77**, 045434 (2008).
[20] M. Fiebig, V. V. Eremenko, and I. E. Chupis, *Magnetoelectric Interaction Phenomena in Crystals* (Kluwer Academic, Dordrecht, 2004).
[21] D. D. Awschalom, D. Loss, and N. Samarth, *Semiconductor Spintronics and Quantum Computation* (Springer-Verlag, Berlin Heidelberg, 2002).
[22] V. N. Golovach, M. Borhani, and D. Loss, Phys. Rev. B **74**, 165319 (2006).
[23] K. C. Nowack *et al.*, Science **318**, 1430 (2007).
[24] K.-Y. Choi *et al.*, Phys. Rev. Lett. **96**, 107202 (2006).
[25] B. Tsukerblat, *Group Theory in Chemistry and Spectroscopy* (Academic, New York, 1994).
[26] W. Wernsdorfer *et al.*, Nature (London) **416**, 406 (2002).
[27] F. Troiani *et al.*, Phys. Rev. Lett. **94**, 190501 (2005).
[28] M. Tavis and F. W. Cummings, Phys. Rev. **170**, 379 (1968).
[29] I. Chiorescu *et al.*, Phys. Rev. Lett. **84**, 3454 (2000).
[30] M. C. Juan *et al.*, Inorg. Chem. **44**, 3389 (2005).
[31] J. Luzon *et al.*, Phys. Rev. Lett. **100**, 247205 (2008).